Langmuir

Article

pubs.acs.org/Langmuir

Influence of Film Composition on the Morphology, Mechanical Properties, and Surfactant Recovery of Phase-Separated Phospholipid-Perfluorinated Fatty Acid Mixed Monolayers

Ala'a F. Eftaiha,[†] Sophie M. K. Brunet,[‡] and Matthew F. Paige*[,†]

[†]Department of Chemistry and [‡]Saskatchewan Structural Sciences Centre, University of Saskatchewan, 110 Science Place, Saskatoon, Saskatchewan, Canada S7N 5C9

Supporting Information

ABSTRACT: Monolayer surfactant films composed of a mixture of phospholipids and perfluorinated (or partially fluorinated) surfactants are of potential utility for applications in pulmonary lung surfactant-based therapies. As a simple, minimal model of such a lung surfactant system, binary mixed monolayer films composed of 1,2-dipalmitoyl-*sn*-glycero-3-phosphocholine (DPPC) and perfluorooctadecanoic acid (C18F) prepared on a simplified lung fluid mimic subphase (pH 7.4, 150 mM NaCl) have been characterized in terms of mixing thermodynamics and compressibility (measured through π–A compression isotherms), film morphology (via atomic force, fluorescence, and Brewster angle microscopy), as well as spreading rate and hysteresis response to repeated expansion–contraction cycles for a variety of compositions of mixed films. Under all mixing conditions, films and their components were found to be completely immiscible and phase-separated, though there were significant changes in the aforementioned film properties as a function of composition. Of particular note was the existence of a maximum in the extent of immiscibility (characterized by ΔG_{ex}^{π} values) and enhanced surfactant recovery during hysteresis experiments at $\chi_{C18F} \geq 0.30$. The latter was attributed to the relatively rapid respreading rate of the perfluorinated amphiphile in comparison with DPPC alone at the air–water interface, which enhances the performance of this mixture as a potential pulmonary lung surfactant. Further, monolayer film structure could be tracked dynamically as a function of compression at the air–water interface via Brewster angle microscopy, with the C18F component being preferentially squeezed out of the film with compression, but returning rapidly upon re-expansion. In general, addition of C18F to DPPC monolayers resulted in improvements to mechanical, structural, and respreading properties of the film, indicating the potential value of these compounds as additives to pulmonary lung surfactant formulations.

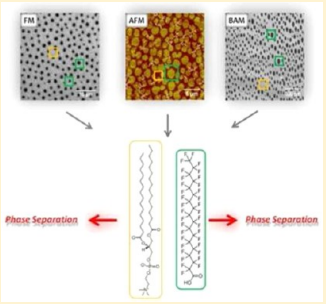

1. INTRODUCTION

Pulmonary lung surfactant (PS), a complex mixture of surfactants and proteins found in the alveoli and affiliated bronchiol surfaces, plays a crucial role in regulating surface tension during normal respiration cycles.[1−3] Production of insufficient or faulty PS has been associated with a variety of disease states, most notably in infants as neonatal respiratory distress syndrome, and similar medical difficulties have been reported in adults following traumatic lung injury. While a complex mixture, the primary lipid component of native PS are phosphatidylcholines (PCs; ∼80% of the total lipid content) such as 1,2-dipalmitoyl-*sn*-glycero-3-phosphocholine (DPPC), whose primary function is to generate stable, low surface tension PS films at the air–alveolar fluid interface, thereby decreasing work associated with lung expansion during respiration. However, this property alone is insufficient to ensure proper lung performance; functionally competent PS must also respread rapidly at the air–alveolar interface (with spreading rates on the same time-scale as respiration rates) and allow for rapid replenishment of the alveolar surfactant layer through formation of surfactant "reservoirs" in the bulk liquid phase.[3] DPPC typically has poor respreading characteristics and as such cannot, alone, serve as a good PS material.

For in vivo PS, the necessary functionality is met through combining diverse types of lipids in addition to various surface-active proteins.[4] There is considerable interest in the development of artificial PS formulations for treatment of respiratory distress syndrome, and a number of these formulations have been approved for medical applications (e.g., Survanta, Infosurf). While useful, many PS formulations are based on animal lung extracts which can suffer from large batch-to-batch variation as well as concerns over potential zoonotic diseases, and there is sufficient motivation to develop purely synthetic PS preparations. Efforts to date in this area have included PS formulations based on mixtures of PCs with various additives to improve surfactant respreading and other performance properties, with additives including primary alcohols, polymers (tyloxapol, dextran, polyethylene glycol), as well as a variety of synthetic or semisynthetic peptides and proteins.[5−9] While the various peptides and proteins contained in PS play an invaluable role in enhancing the performance of

Received: July 3, 2012
Revised: September 17, 2012
Published: October 8, 2012

PS, their use significantly increases material costs and creates handling challenges with these formulations.

Fluorinated and semifluorinated surfactant additives have recently been explored for applications in tailoring properties of potential PS mixtures.[10−13] Fluorinated surfactants are highly surface-active materials that can yield air−water surface tensions that are less than those obtained with conventional hydrocarbon-based surfactants. The compounds tend to be chemically stable over a wide range of conditions and are often used in combination with their hydrogenated counterparts to achieve lower surface tensions, and to improve liquid spreading and chemical robustness.[14,15] Fluorinated surfactants can be miscible, partially miscible or entirely immiscible with hydrogenated surfactants, depending on the precise chemical nature of the chemical system, and while they can be useful additives for various surfactant applications, great care must be taken in order to fully optimize the performance of mixed fluorocarbon−hydrocarbon mixtures because of these miscibility issues. Further, for some fluorinated surfactants, there are significant concerns related to their toxicity and propensity for bioaccumulation, both of which are of particular importance for medical applications.[14,16] Nonetheless, fluorinated surfactants are technologically useful and potentially beneficial additive molecules for tailoring properties of PS formulations. As such, characterizing simple, minimal model monolayer systems composed of PCs mixed with perfluorinated additives on lung fluid mimic subphases is of significant interest for formulating potential artificial PS mixtures.

Properties of mixed PC-fluorinated surfactant monolayer films have been investigated via Langmuir and Langmuir−Blodgett (LB) approaches by a number of groups and under various mixing conditions. Lehmler and Bummer[17,18] have investigated the miscibility and film-forming capabilities of monolayer mixtures of PCs and semifluorinated surfactants and found that the extent of surfactant miscibility depended strongly upon differences in surfactant chain lengths (increasing the length of constituent molecules above a certain size resulted in increased immiscibility), headgroup charge (opposite charges on head groups leads to increased miscibility), and surface pressure. Hoda and co-workers[19,20] have reported monolayer studies of the interaction between hybrid fluorinated-hydrogenated surfactants and DPPC, in which it was found that the hybrid amphiphiles were generally miscible with PC and could effectively fluidize and disperse liquid-condensed domains of the phospholipid. Similar results were described by Courier et al.[21] and Hiranita et al.[22] for closely related systems.

Of particular interest to our research group have been efforts aimed at characterizing miscibility and monolayer structures of DPPC mixed with simple perfluorocarboxylic acids; Nakahara et al.[23,24] have surveyed the miscibility of a number of perfluorocarboxylic acids (C*n*F, *n* = 12, 14, 16, 18) with DPPC; while Yokoyama et al. have investigated dipalmitoylphosphatidylglycerol (DPPG) and dimyristoylphosphatidylethanolamine (DMPE) phospholipids on a low pH, high salinity subphase (pH = 2.0, 150 mM NaCl).[25,26] Similar to the systems described above, the degree of miscibility depended strongly on the surfactant chain length as well as the relative mole fraction of perfluorocarboxylic acid; addition of C12F to DPPC resulted in efficient fluidization of the phospholipid, but the effect was reversed (domain solidification) for longer perfluorocarbon chains. In the case of DPPC-C18F, mixtures were found to be highly immiscible, resulting in phase-separated domains in both Langmuir and LB films as observed by fluorescence microscopy and atomic force microscopy. Research in our own laboratory has shown that the extent of miscibility of C18F and DPPC is a strong function of subphase pH and sodium ion concentration, with the system forming miscible, unstructured films at pH = 5.5 and ion concentrations ranging from nominal zero to 400 mM.[11] Specific adsorption of ions to the negatively charged headgroups of C18F under these conditions led to a decrease in the net attractive interactions between film components via headgroup interactions, resulting in a lessening of the cohesive force within the films.

While the combined works described above have provided valuable insight into basic thermodynamic and structural properties of mixed dialkylphosphatidylcholine-C18F monolayer films, there are many important issues relating to performance of these mixtures as potential PS replacement systems, even when considering these binary systems as simple minimal models. In this work, we present an in-depth investigation of the mixing thermodynamics, spreading kinetics, film morphology (at both the solid−air and liquid−air interfaces), and film hysteresis after multiple compression−expansion cycles for mixed monolayers composed of DPPC and C18F (chemical structures shown in Scheme 1). Sample films have been prepared using a highly simplified lung fluid (pH 7.4, 150 mM NaCl) as an aqueous subphase to mimic some of the properties of alveoli and bronchial space, though we note that the actual in vivo environment will contain a significantly more complicated mixture of inorganic ions, proteins, and affiliated chemical species. To our knowledge, this is the first report of a combined thermodynamic, kinetic, and structural characterization of a mixed DPPC-C18F monolayer film under subphase conditions relevant to pulmonary lung surfactant applications. Results indicate that while the two film components are immiscible, addition of the perfluorocarboxylic acid can cause significant alterations (and in some cases, enhancements) to film properties that are useful in PS applications, including both unique structural changes and enhanced spreading kinetics that have not been previously reported, and that use of these perfluorinated amphiphiles holds some considerable potential as additives for these formulations.

Scheme 1. Chemical Structures of (A) DPPC; (B) C18F; and (C) Bodipy-PC

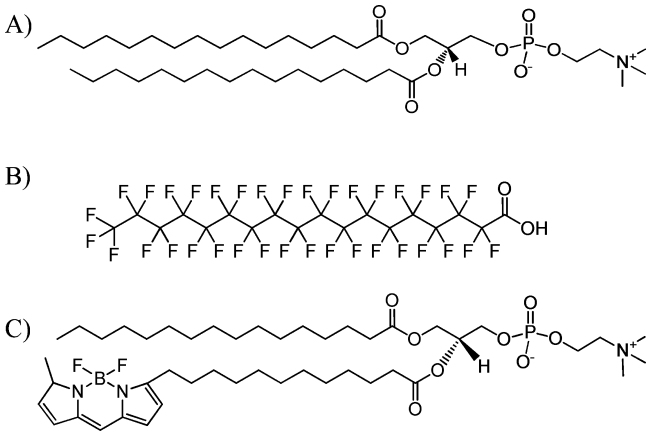

dx.doi.org/10.1021/la3026655 | *Langmuir* 2012, 28, 15150−15159

2. MATERIALS AND METHODS

2.1. Chemicals. The surfactants DPPC and C18F were purchased from Avanti Polar Lipids and Alfa Aesar, respectively, and used as received. The fluorescent probe, 2-(4,4-difluoro-5-methyl-4-bora-3a,4a-diaza-*s*-indacene-3-dodecanoyl)-1-hexadecanoyl-*sn*-glycero-3-phosphocholine (Bodipy-PC; structure shown in Scheme 1C) was purchased from Invitrogen Corp. The *n*-hexane, methanol (MeOH), and sodium chloride were purchased from Fisher Scientific, while chloroform ($CHCl_3$) and sodium hydroxide was purchased from EMD Canada. Microscope cover glass and muscovite mica were from VWR International and Structure Probe Inc., respectively. Mica was freshly cleaved with adhesive tape prior to use, while the microscope cover glass was rinsed thoroughly with ethanol, dried under nitrogen gas, and cleaned in a plasma cleaner (Harrick Plasma) to remove any residual contaminants.

2.2. Surface Pressure−Area Isotherms. Stock solutions of DPPC and C18F were prepared by dissolving the solid surfactants in 8:1:1 and 7:1:2 volume ratio of hexane/$CHCl_3$/MeOH, respectively. The solutions were combined in appropriate volumes to give the desired molar ratio of surfactants. Surface pressure−mean molecular area (π−A) isotherms were measured in a Langmuir trough (mini-trough, KSV NIMA.), with surface pressure monitored using a Wilhelmy balance and paper Wilhelmy plate. A minimum of three independent isotherms were run for each composition of film, and the isotherms displayed in figures are the means of these experiments. Ultrapure water (Millipore, resistivity 18 MΩ·cm) was used to prepare a subphase of 150 mM NaCl. The pH of the subphase was adjusted with 70 mM NaOH to 7.4 ± 0.2. An aliquot of the amphiphile solution was spread on the subphase surface at 25 ± 1 °C, with temperature controlled using an external circulating water bath. The solvent was allowed to evaporate for 10 min before the monolayer was compressed at a speed of 1000 mm·min^{-1} (570 Å^2·molecule^{-1}·min^{-1}). Film hysteresis and surfactant recovery was measured by recording five successive compression−expansion cycles with no lag time between consecutive cycles, with the expansion rate equal to the compression rate (1000 mm·min^{-1}).

2.3. Langmuir−Blodgett (LB) Film Deposition. LB films were prepared for a 0.5 C18F mole fraction (χ_{C18F}) mixture using a Langmuir trough (standard trough, KSV NIMA) and the subphase conditions described above. After surfactant spreading and solvent evaporation, films were compressed at a rate of 20 mm·min^{-1} (11.4 Å^2·molecule^{-1}·min^{-1}) until reaching a surface pressure of 2 mN/m. The film was allowed to stabilize for 10 min, and the substrate (mica for AFM imaging or cover glass for fluorescence imaging) was pulled upward through the water−air interface in a single stroke. The film was left to dry in a clean environment at room temperature for several hours before measurements. For samples used in fluorescence imaging experiments, an aliquot of Bodipy-PC solution (fluorescent probe was dissolved in 8:1:1 volume ratio of hexane/$CHCl_3$/MeOH) was added to the surfactant mixture to give a final fluorescent probe concentration of 2.1 × 10^{-3} mol % (ratio of Bodipy-PC to the total amount of amphiphile).

2.4. Microscopy Measurements. For Brewster angle microscope (BAM) measurements, an aliquot of surfactant solution was spread over the subphase in a Langmuir trough and the solvent was allowed to evaporate. The monolayer was then compressed at 20 mm·min^{-1} (11.4 Å^2/molecule·min^{-1}) to the desired surface pressure. The monolayer was measured using a KSV NIMA UltraBAM system (KSV NIMA). The microscope used a 50 mW, 658 nm polarized laser as an illumination source and a CCD detector (collection rate of 20 frames/s). The lateral resolution of the instrument was 2 μm (based on the Rayleigh criterion), and the angle of the incident beam to the air−water interface was fixed to the Brewster angle (53.1°).

Atomic force microscope (AFM) measurements were carried out on a Dimension Hybrid Nanoscope system (Veeco Metrology Group), operating in contact mode in air using silicon nitride AFM probes ($k \sim$ 0.1 N·m^{-1}), a scan rate of 0.5 Hz, and 512 pixels/line. Samples could be imaged repeatedly without apparent tip-induced damage.

Bodipy-PC doped films were imaged in a modified LSM-410 Zeiss laser scanning confocal microscope (LSM Tech), using the 457 nm excitation laser line of an argon ion laser. Fluorescence emission was filtered with a 500 nm long-pass filter.

All microscope images shown are representative examples; measurements of different regions of the same film and different samples gave comparable results.

3. RESULTS AND DISCUSSION

Surface pressure−area isotherms were measured at 25 °C for the pure individual surfactants as well as their mixtures, with resulting isotherms shown in Figure 1. Isotherms for the pure components were consistent with those reported elsewhere in the literature, with the pure DPPC isotherm exhibiting characteristic gaseous, liquid-expanded (LE), and liquid-condensed (LC) phases, with coexistence regions and a collapse plateau of ∼66 mN/m, and the C18F isotherm exhibiting a single, smooth curve with collapse plateau of ∼64 mN/m.[11,27] Limiting molecular areas (A_0) for the pure components, estimated by extrapolating the pseudolinear portion of the liquid-condensed phase to the mean molecular area axis intercept, were ∼61 and ∼34 Å^2·molecule^{-1} for DPPC and C18F, respectively. As an aside, Nakahara and Shibata[24] have commented that perfluorocarboxylic acids from commercial sources can contain significant impurities (certified purity of C18F from Alfa Aesar used here was reported as ∼97%) and have suggested that these impurities can result in A_0 values that are unreasonably large in comparison with those estimated from the cross-section of a perfluorocarbon chain (∼28 Å^2). Further, the authors suggest that multiple recrystallizations of these materials are necessary for meaningful quantitative measurements. In this work, π−A isotherms for commercial C18F gave A_0 values that were larger than those reported for Nakahara's highly purified compounds (34 vs 29 Å^2·molecule^{-1}), though careful inspection of the literature indicates that even for nominally purified C18F a sizable range of A_0 values can be found. We have measured isotherms after performing multiple recrystallizations (following a similar procedure to that described by Tsuji et al.[28]) of the commercial C18F, and the isotherms were, within error, the same as those from the commercial product. ^{19}F-NMR spectra for both the commercial and recrystallized compound were the same and indistinguishable from those of a model compound perfluorooctanoic acid,[29] and no spectral peaks that might be attributed to impurities were observed (see the Supporting Information). Finally, the melting point of the commercial C18F was 168 °C, in comparison with the range of 162−164 °C Nakahara has reported for impure surfactant. In combination, we take these measurements as indicating that the commercial C18F used in this study had an acceptably high degree of purity for quantitative measurements and further purification was not necessary.

Isotherms for the surfactant mixtures were similar in appearance to the pure C18F isotherms, and consisted of a single, smooth curve with no LE-LC coexistence regions. This is consistent with previous observations under different subphase conditions, in which the addition of perfluorocarboxylic acids to DPPC results in fluidization of LC domains, and it is likely that the same action is in effect under these conditions. Addition of C18F to DPPC resulted in a shift in the isotherms at low pressures to a higher mean molecular area in comparison to DPPC alone, with the extent of the shift increasing as a function of the relative proportion of C18F. Further, mixed

dx.doi.org/10.1021/la3026655 | Langmuir 2012, 28, 15150−15159

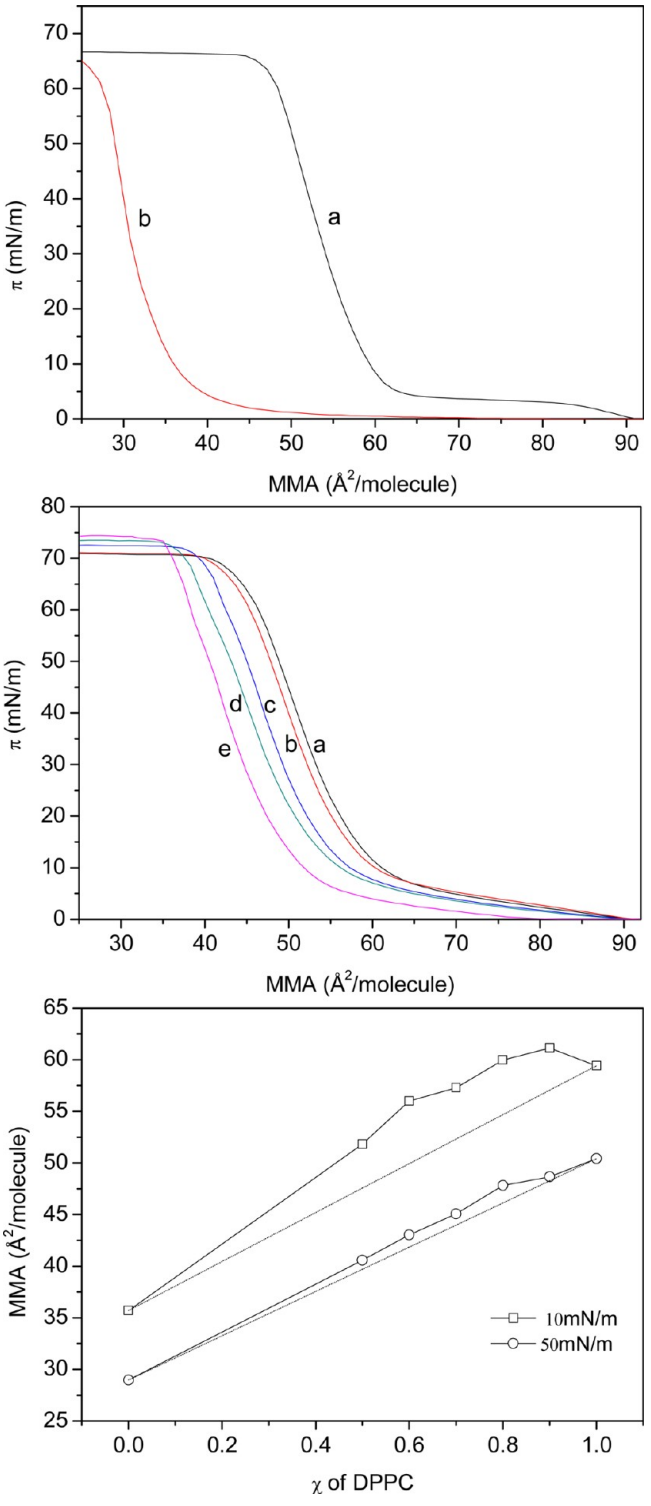

Figure 1. (A) π–A isotherms for (a) pure DPPC and (b) pure C18F monolayer films on pH 7.4, 150 mM NaCl subphase. (B) π–A isotherms for (a) χ_{C18F} = 0.1; (b) χ_{C18F} = 0.2; (c) χ_{C18F} = 0.3; (d) χ_{C18F} = 0.4; and (e) χ_{C18F} = 0.5 mixed monolayer films. (C) Mean molecular area as a function of mole fraction of DPPC (□, 10 mN/m; ○, 50 mN/m). The dashed lines represent ideal mixing behavior as predicted by eq 1, and the solid lines are a guide to the eye.

monolayers showed significant positive deviations from ideal mixing (Figure 1C) predicted by the two-component additivity relationship described in eq 1:[30]

$$A_{12} = A_1\chi_1 + A_2\chi_2 \quad (1)$$

where A_1, A_2 are the mean molecular areas of the individual film components for a given surface pressure, A_{12} is the mean molecular area of the mixed film, and χ_i is the mole fraction of the ith component in the mixture.

All mixed films showed positive deviations from ideal mixing, indicating the existence of significant repulsive interactions between the film components,[30] though the extent of these deviations decreased significantly with increasing surface pressure. Relative uncertainties in these measurements were small and are documented in the Supporting Information. Previous reports of DPPC-C18F miscibility by Nakahara et al.[23,24] and our group[11] under different subphase conditions (pH 2, 150 mM NaCl and pH 5.5, 0–400 mM NaCl, respectively) have observed negative deviations from ideality (attractive interactions between components), with the effect being ascribed to attractive interactions between the oppositely charged headgroups (zwitterionic choline headgroup for DPPC and negatively charged carboxylate for C18F) under the subphase conditions used.

It is instructive to consider the influence of pH on the extent of ionization of C18F for the different experimental conditions described above; the degree of ionization of C18F in the monolayer can be estimated through eq 2, based on the Boltzmann distribution of ions in an electric field and the Gouy–Chapman model of charged interfaces:[24,30]

$$\mathrm{pH}_{\mathrm{bulk}} = \mathrm{p}K_a + \log\frac{\alpha}{1-\alpha} + 0.87\sinh^{-1}\left(\frac{1.37\alpha}{A\sqrt{c}}\right) \quad (2)$$

where K_a is the acid dissociation constant, α is the fractional ionization of the acid, A is the surface film area on a per molecule basis, and c is the molar concentration of electrolyte.

Assuming a pK_a of 2.8 for C18F (estimated from closely related compounds[14]), then a gaseous film of C18F has $\alpha \sim$ 99% at bulk subphase pH = 7.4 as compared to ~9% for pH = 2.0. One can reasonably argue that, for a pH = 2.0 subphase, the small subpopulation of negatively charged C18F molecules will interact electrostatically with the zwitterionic headgroups of DPPC, resulting in the observed film stabilization. However, this cannot explain the results at elevated pH because if this were the dominant effect, the film would be further stabilized, not destabilized. It appears that the principle source of this effect is the role played by sodium ion; we have previously demonstrated that sodium ion in the subphase decreases electrostatic interaction between the two film components through specific adsorption to the carboxylate headgroup,[11] and this effect will be of even greater importance since the number of available sodium ion adsorption sites is approximately 10-fold larger at pH 7.4. Negation of the headgroup–headgroup stabilization interaction through specific ion-binding, in combination with repulsion between the alkyl and perfluorinated chains, results in a net repulsive interaction between components.

The extent of film stabilization (or destabilization) due to interactions between film components can be evaluated from the isotherm data by calculating excess Gibbs free energies of mixing (ΔG_{ex}^{π}) via eq 3:

$$\Delta G_{ex}^{\pi} = \int_{\pi}^{0} [\sigma_{12} - (\chi_1\sigma_1 + \chi_2\sigma_2)]\,\mathrm{d}\pi \quad (3)$$

where σ_i is the molar area of the pure film and σ_{ij} is the molar area of the mixed film.

dx.doi.org/10.1021/la3026655 | Langmuir 2012, 28, 15150–15159

Positive or negative excess values of the Gibbs excess function indicate either repulsive or attractive interactions. As shown in Figure 2 below, the mixed monolayer systems showed

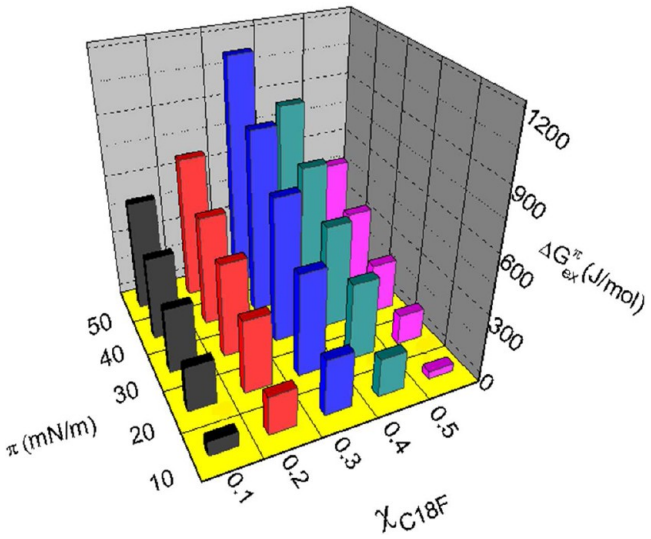

Figure 2. Plot showing excess Gibbs free energies of mixing (ΔG^{π}_{ex}) as a function of film composition and subphase pressure for the mixed monolayer films on pH 7.4, 150 mM NaCl subphase.

positive ΔG^{π}_{ex}, with values ranging from 0.1 to 0.9 kJ·mol^{-1}, indicating a significant nonideal repulsive interaction between components for all compositions. Values for ΔG^{π}_{ex} were found to increase as a function of increasing C18F, until reaching a maximum at a mixing ratio of χ_{C18F} = 0.3, followed by a decrease in magnitude at greater C18F fraction, and also increased with increasing surface compression, which can be attributed to an increasing importance of short-range repulsive forces in close-packed films.[19] To provide a "calibration" scale, these are modestly small repulsive interactions in comparison with thermal energy (RT ~ 2.5 kJ·mol^{-1}), and only slightly larger than the estimated contribution to film stabilization energy from the headgroup−headgroup interaction between DPPC and the perfluorcarboxylic acid (~0.25 kJ·mol^{-1}).[31] Hoda et al.[20] have reported comparable magnitude (and sign) interaction energies (calculated via the Joos equation) between DPPC and hybrid fluorocarbon−hydrocarbon hexylphosphate surfactants, though negative ΔG^{π}_{ex} values on the order of −0.1 to −0.8 kJ·mol^{-1} were reported by Nakamura et al.[32] for mixtures of DPPC with single-chain (perfluorooctyl)pentanol and (perfluorooctyl)pentylphosphocholine. In short, significant changes to the chemical nature of the perfluorinated surfactant typically have modest, though significant effects upon overall film stability, allowing control over the film miscibility from being ideally to entirely nonideally miscible. For the simple surfactants and lung surfactant mimicking subphase conditions used here, it appears that the repulsive contributions to overall film stability arising from hydrocarbon−perfluorocarbon tail group interactions dominate any net attractive interaction resulting from headgroups. The effect is particularly important at χ_{C18F} ~ 0.3 which, as will be shown in upcoming sections, results in the formation of a highly structured surfactant film.

To assess mechanical properties of the mixed monolayer films at the air−water interface, isothermal compressiblities (C_s) have been determined via eq 4 and are summarized for control samples of pure DPPC, C18F, and their mixed films (χ_{C18F} = 0.1−0.5) at four different surface pressures in Table 1:

$$C_s = -\left(\frac{1}{A}\right)\left(\frac{dA}{d\pi}\right) \quad (4)$$

where A is the mean molecular area determined from the surface compression isotherms.

Isothermal compressibility values provide information on the degree of film elasticity; condensed, rigid DPPC films yield small values of C_s (a more elastic film), and as such the values can be used to assess the degree of monolayer elasticity upon addition of perfluorocarbons. Desirable compressibility values of PS films are typically <0.01 (mN/m)$^{-1}$, meaning minimal lung compression (typically 20−30% area reduction[3]) is needed to affect a physiologically appropriate decrease in surface tension. Pure films of C18F gave larger C_s values than pure DPPC under all film compression values, though the difference was minimal at the highest extent of compression (40 mN/m; both films are in the condensed phase under these conditions). Mixtures of the two components gave C_s values that were comparable to those of pure C18F films for the majority of compositions measured. At each fixed surface pressure, there were some minor variations in C_s as a function of χ_{C18F}, but when accounting for standard deviations there was no readily discernible trend to the variations, and we simply report mean values of C_s for all mixtures at a fixed pressure here. The minimum values of C_s (the most elastic film) over the conditions explored were ~4×10^{-3} (mN/m)$^{-1}$, but overall the elasticity was not particularly sensitive to the total amount of C18F in the mixture. In terms of absolute C_s values, Zuo et al.[33] have reported values for bovine lipid extract surfactant (BLES; mixtures of native surfactants plus SP-B, SP-C, two principal surfactant proteins) on the order of 1.5×10^{-2} (mN/m)$^{-1}$ over the surface pressure range studied here, while Wuestneck et al.[34] and Aydogan et al.[10] have reported minimum values of 3×10^{-3} (mN/m)$^{-1}$ for DPPC SP-C mixtures and DPPC mixed with a novel hydrocarbon−fluorocarbon hybrid cationic amphiphile, respectively (latter two groups measured values via pendant drop-surface dilational approaches). In the case of Aydogan's measurements, addition of low levels of fluorosurfactant significantly increased film elasticity of the mixed films over DPPC alone, though this was not the case here with C18F.

Table 1. Isothermal Compressibility (mN/m)$^{-1}$ Values for Pure and Mixed Surfactant Monolayers on the pH 7.4, 150 mM NaCl Subphase at 25 °C

	C_s (mN/m)$^{-1}$			
surfactant	π = 10 mN/m	π = 20 mN/m	π = 30 mN/m	π = 40 mN/m
pure components				
DPPC	$(6.7 \pm 0.3) \times 10^{-3}$	$(4.5 \pm 0.1) \times 10^{-3}$	$(3.7 \pm 0.1) \times 10^{-3}$	$(3.5 \pm 0.1) \times 10^{-3}$
C18F	$(1.2 \pm 0.1) \times 10^{-2}$	$(7.0 \pm 1) \times 10^{-3}$	$(4.6 \pm 0.3) \times 10^{-3}$	$(3.6 \pm 0.2) \times 10^{-3}$
mixtures of χ_{C18F} = 0.1−0.5	$(1.4 \pm 0.2) \times 10^{-2}$	$(6.8 \pm 0.5) \times 10^{-3}$	$(5.1 \pm 0.5) \times 10^{-3}$	$(4.5 \pm 0.3) \times 10^{-3}$

dx.doi.org/10.1021/la3026655 | Langmuir 2012, 28, 15150−15159

It should also be noted for C18F, however, that while perfluorocarbon addition minimally alters C_s, absolute values are still well within the range required for a competent PS mixture, and mechanical properties of DPPC films at the air−water interface are not unduly perturbed by addition of the perfluorocarbon component.

In addition to examining the effect of C18F addition upon the thermodynamic and mechanical properties of the DPPC monolayer, we have also carried out preliminary measurements of surfactant spreading rates on the simplified lung-fluid mimic subphase. This is a particularly important property for PS performance as noted above, as the surfactant needs to rapidly respread over alveolar surfaces during respiration cycles. Measurements were carried out using a modified version of Taeusch's approach,[35] in which a circular Teflon dish (6 cm diameter) was filled with subphase, an aliquot of surfactant solution was deposited onto the subphase via microsyringe, and surface pressure was monitored as a function of time immediately after deposition (distance between addition point and Wilhelmy plate was ∼3 cm). Spreading data is shown in Figure 3 for the pure individual components as well as

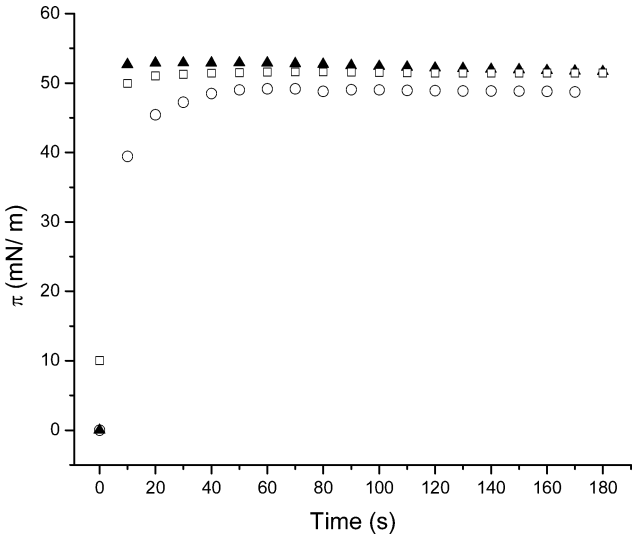

Figure 3. Surface pressure measured as a function of time for spreading of surfactants on the pH 7.4, 150 mM NaCl subphase (▲, C18F; □, χ_{C18F} = 0.2; ○, DPPC).

for a representative mixture (χ_{C18F} = 0.2). The rate of spreading for the C18F was faster than the time resolution of our measurements, with the film reaching its equilibrium spreading pressure (π_{eq} ∼ 53 mN/m) almost immediately upon surfactant addition (<10 s). DPPC films spread significantly more slowly than the C18F, attaining equilibrium (π_{eq} ∼ 50 mN/m) in ∼40 s. The rate of spreading of the pure DPPC on the lung mimic subphase is comparable though slightly faster than that reported for the spreading of several different aqueous surfactant suspensions (native and extracted porcine surfactant as well as the commercial clinical surfactants Curosurf, Survanta, and Infasurf) in the presence of serum, which typically attain π_{eq} ∼ 40 mN/m in approximately 2 min (with spreading rates a strong function of subphase conditions).[35] Measurements were made for a variety of mixed films, and while addition of C18F to DPPC generally resulted in more rapid spreading (∼20 s to reach equilibrium), there was significant variability in the data (possibly due to difficulties in adding the surfactant droplet to precisely the same position in the Teflon dish for each measurement). Because of this and the relatively modest time resolution of the measurements, we have not attempted a more quantitative evaluation of the kinetic data, but simply report that, under subphase conditions that mimic lung surfactant fluid, the addition of C18F results in a more rapid (approximate doubling) decrease in surface tension over DPPC alone.

It is worth noting that one of the primary protein components of native PS, SP-C, likely working in conjunction with other peptides, is believed to play a key role in improving surfactant respreading rates for in vivo PS mixtures. Pastrana et al.[36] have reported that addition of bovine extracted SP-C to DPPC-DPPG surfactant mixtures results in 50-fold faster surfactant spreading rates (500 min improved to 10 min). Other additives (palmitic acid, hexadecanol) can have similar effects. While spreading rate improvements offered by C18F are significantly more modest than those offered by SP-C, they are nonetheless significant and the costs and handling issues associated with use of peptides or animal extracts are considerable. This suggests that addition of the perfluorinated surfactant to DPPC can improve not only overall surface tension values, but also kinetic performance of mixed surfactant films for PS applications, without the challenges associated with use of proteins and peptides. However, we note that caution must be taken when interpreting spreading data (measuring surface pressure after direct addition of surfactant to air−water interface) in the context of surfactant respreading after film collapse, which is a more appropriate descriptor of what takes place at the alveolar surface during respiration. The latter likely requires fusion of surfactant bilayers or micelles to the interface,[3] and measuring simple spreading rates is clearly a crude approximation of a more complex kinetic process. Nonetheless, as will be shown below through BAM measurements, respreading of surfactants from collapsed films occur on the time-scale of seconds, suggesting that these measurements, while clearly approximations, are reasonable ones and capture the essence of the surfactant respreading process.

A combination of surface microscopy techniques, including BAM imaging, AFM imaging, and laser scanning confocal microscope imaging, were used to structurally characterize the mixed film samples and to probe dynamics of the films under compression. BAM images of the pure DPPC and mixed monolayer films at the air−water interface are shown in Figure 4. We note that the refractive index for typical perfluorocarbons is similar to that of pure water (at 25 °C, n_{water} ∼ 1.33, $n_{perfluorocarbon}$ ∼ 1.40[37]) and dark regions (low reflectivity) in BAM images correspond to water, perfluorocarbon, or a mixture of both (images of pure C18F films are featureless). We further note that image morphology appears different for all three techniques, as they generate contrast by entirely different mechanisms (reflectivity, morphology, and the presence of a fluorescent probe, respectively). As reported elsewhere (see McConnell,[27] for example,) images of low surface pressure DPPC films exhibited minimal features up to the coexistence LE-LC region (data not shown), whereupon characteristic multilobed, condensed domains were abundant (Figure 4A). Further film compression lead to an increase in the area occupied by these domains until spacing between domains could not be spatially resolved by the microscope and images appeared unstructured. Addition of C18F to the DPPC films led to morphological variations in the mixed film structures.

dx.doi.org/10.1021/la3026655 | *Langmuir* 2012, 28, 15150−15159

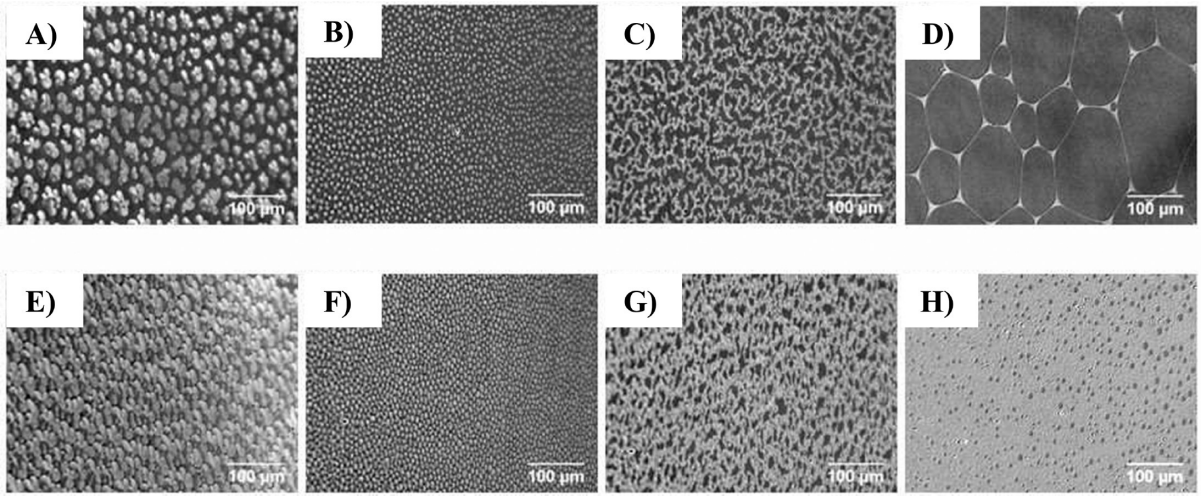

Figure 4. Brewster angle micrographs (620 μm × 340 μm) of monolayer films at the air−water interface: (A) DPPC; (B) χ_{C18F} = 0.1; (C) χ_{C18F} = 0.2; (D) χ_{C18F} = 0.5; (E) DPPC; (F) χ_{C18F} = 0.1; (G) χ_{C18F} = 0.2; and at 64 Å^2/molecule; (H) χ_{C18F} = 0.5. Films in (A)−(D) were compressed to an area of 70 Å^2/molecule, and those in (E)−(H) were compressed to an area of 60 Å^2/molecule.

Films containing χ_{C18F} = 0.1 (Figure 4B) exhibited numerous condensed domains (diameter ∼ 8 μm vs 35 μm for pure DPPC), with the characteristic lobe-structure of the LC domains being replaced with circular domains. The shift from lobed-structure to circles is consistent with the minimization of line-tension at the phase-boundary between coexisting perfluorocarbon and hydrocarbon phases, and is also consistent with the expected fluidization of the condensed DPPC described in the isotherm data. Morphologies continued to change with increasing χ_{C18F}. At χ_{C18F} = 0.2 (Figure 4C), extended interwoven strands were observed, with dark regions occupying the space between strands. The most dramatic morphological changes were observed for $\chi_{C18F} \geq 0.3$ (representative image shown in Figure 4D; other values of χ_{C18F} gave comparable images). Films prepared with these compositions consisted of a meshlike network of reflective surfactant (DPPC) surrounding dark, discrete, discontinuous domains. These are the same compositions at which maximum nonideal mixing behavior was observed in the ΔG^{π}_{ex} values, and it is clear that the film components are fully phase-separated. Further compression of the films (Figure 4H) results in a net decrease in separation of the highly reflective domains, or in the case of $\chi_{C18F} \geq 0.3$ a decrease in the total area occupied by the dark (perfluorocarbon) domains, and in subsequent sections particular attention will be paid to the meshlike network in terms of structure and hysteresis response to compression−expansion cycles. In combination, we take these results to mean the DPPC-C18F mixtures are fully immiscible over the composition ranges and subphase conditions measured here, with the degree of repulsive interactions between film components giving rise to significant alterations in overall film morphology at the air−water interface.

Further molecular-scale morphology and compositional information about the mixed films can be collected through AFM and laser scanning confocal measurements. We have chosen to focus attention on the most highly structured, phase-separated films that form at $\chi_{C18F} \geq 0.3$. LB films of χ_{C18F} = 0.5 on mica were measured in the AFM, and are shown with a cross-sectional analysis in Figure 5. The image reveals the formation of well-defined domains that were roughly circular in shape, typically around 1−2 μm in diameter, surrounded by a

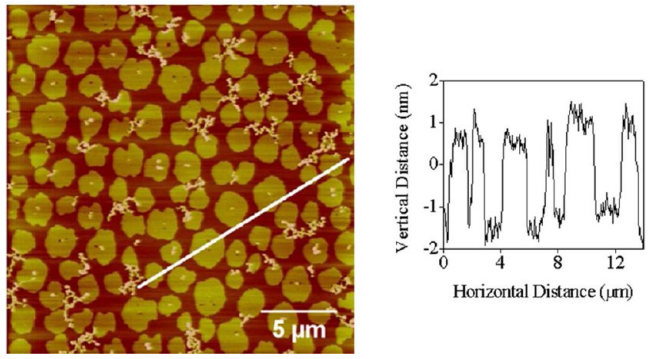

Figure 5. AFM height mode image (20 μm × 20 μm) and cross-sectional analysis of a χ_{C18F} = 0.5 mixed monolayer film deposited on a mica substrate (deposition pressure of π = 2 mN/m) from a subphase of 150 mM NaCl (pH 7.4) at 25 °C.

continuous matrix that was lower in height than the circular domains by 2.0−2.5 nm. Nanometer-scale deposits, likely crystallized salt from the high salinity subphase, were occasionally observed, though these did not significantly obscure the underlying film morphology.

The average difference in height between the circular domains and the surrounding matrix was comparable to the fully extended molecular length of either DPPC (2.8 nm) or C18F (2.5 nm).[38,39] The BAM and AFM images show a film structure that consists of a continuous matrix and numerous discrete patches. The low reflectivities of the circular domains in the BAM images indicate that they are comprised of perfluorocarbon. In combination with the AFM, this suggests that the circular domains are vertically adsorbed C18F, with the surrounding continuous matrix consisting of DPPC lying flat on the underlying substrate. This interfacial organization suggests the film components are fully separated. For additional verification of this assignment and molecular-level organization of the films, samples were doped with Bodipy-PC (Scheme 1C), a fluorescent DPPC analogue, and imaged using confocal fluorescence microscopy. Bodipy-PC partitions preferentially into the LE phospholipid phase (see, for example, Korlach et al.[40]), and we note that at the deposition pressures used here (π = 2 mN/m), the phospholipid film should consist almost

dx.doi.org/10.1021/la3026655 | Langmuir 2012, 28, 15150−15159

exclusively of LE phase. Figure 6 shows a confocal fluorescent image of χ_{C18F} = 0.5 mixed film doped with Bodipy-PC and

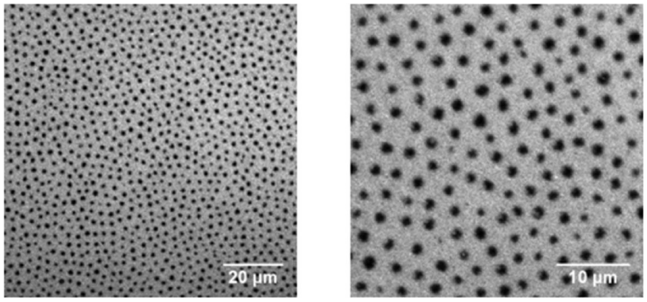

Figure 6. Confocal fluorescence images: (A) 100 μm × 100 μm and (B) 40 μm × 40 μm of χ_{C18F} = 0.5 mixed film doped with Bodipy-PC and deposited onto a glass substrate (deposition pressure of π = 2 mN/m) from a subphase of 150 mM NaCl (pH 7.4) at 25 °C.

deposited on a glass substrate. Images showed the same characteristic surface patterns observed previously in the BAM and AFM images, consisting of a uniform bright background, with a series of discontinuous dark patches (1−2 μm in size).

Because of the preferential partitioning of Bodipy-PC to the LE phase, the highly luminescent continuous matrix must consist of LE DPPC, which is again consistent with the AFM results; phospholipids in the LE phase do not adsorb vertically to the underlying substrate, but will rather lie flush with the surfaces, and the immiscible, phase-separated patches of C18F adopt a close-packed, vertical arrangement.

Surfactant recovery (monolayer hysteresis) of monolayer films after repeated compression−expansion cycles is an important property of PS, with the ability to rapidly and efficiently replenish the surface layer after film collapse being a key performance parameter for these mixtures. In brief, when films are compressed past the collapse pressure (or squeeze-out pressure for one particular component), surfactant is forced into the subphase and may or may not be able to return to the air−water interface upon subsequent re-expansion. Monolayer hysteresis can be evaluated quantitatively by measuring the change in integrated area for π−A isotherms during repeated compression−expansion cycles performed on the Langmuir trough. In these experiments, films were compressed at a fixed rate (1000 mm·min^{-1}; five compression−re-expansion cycles in total) until film collapse (~70−75 mN/m; see Figure 1B), followed immediately by re-expansion at the same rate. Percentage surfactant recovery was defined as

$$\%\ \text{recovery} = \frac{\text{area under isotherm curve for } n\text{th compression cycle}}{\text{area under isotherm curve for 1st compression cycle}} \times 100\% \quad (5)$$

Results of surfactant recovery measurements for the pure films and their mixtures are summarized in Table 2. While all films exhibited some irreversible loss of surfactant, both the pure C18F monolayer and the mixed monolayers with $\chi_{C18F} \geq 0.3$ showed superior percentage recovery in comparison with pure DPPC alone. The recovery data for pure DPPC films highlights one of the shortcomings of the phospholipid as a PS component: its substantial, irreversible loss after the first compression cycle. This effect is likely related to the inability of DPPC vesicles (formed after film collapse) to 'unzip' and rapidly readsorb to the liquid interface after re-expansion.[3]

For C18F, it is reasonable to postulate that recovery is superior to pure DPPC because of the nature of the aggregates that form upon film collapse. Thunemann and Schnablegger[38] have estimated the critical micelle concentration of C18F at ~8 × 10^{-5} mol/L, which is several orders of magnitude larger than that for DPPC (0.46 × 10^{-9} mol/L, Avanti Polar Lipids). After film collapse, the C18F is not expected to form micelles and therefore can be reintegrated into the air−water interface with greater efficiency than micellar DPPC. Increasing the amount of C18F in the mixed films will generally result in increased overall recovery because of this effect. On the basis of the cumulative data, we propose the following model of film dynamics for the immiscible films during compression−expansion cycles: after initial spreading at constant surface area, the immiscible film components are phase-separated at the air−water interface. During compression, the phase-separated domains of C18F are reduced in area (as per Figure 4D and H, for example) until the system approaches the collapse pressure for the film, at which point the C18F will be preferentially forced out of the monolayer (collapse pressure for C18F is marginally lower than that of the DPPC), leaving the film temporarily enriched in DPPC until it, too, is squeezed out into the underlying suphase. Upon re-expansion, the squeezed out C18F component returns back first with reasonably high efficiency, followed, more slowly, by the DPPC component. As the film re-expands, both components are replenished at the air−water interface, though some fraction of both DPPC and C18F are permanently lost to the subphase. We note that this mechanism is consistent with the so-called "squeeze-out" hypothesis for PS operation,[3] in which fluid, non-DPPC PS components are squeezed out of the film during the course of film compression, leaving DPPC (with the assistance of the various protein components of PS) to maintain low π at low surface area values. While the squeeze-out hypothesis mechanism of operation for native PS is actively under debate,

Table 2. Percent Recovery of Mixed Monolayers Compressed Past Their Collapse Pressure as a Function of Consecutive Compression−Expansion Cycles[a]

	percentage recovery (%)						
no. of compression cycles	DPPC	χ_{C18F} = 0.1	χ_{C18F} = 0.2	χ_{C18F} = 0.3	χ_{C18F} = 0.4	χ_{C18F} = 0.5	C18F
2	34 ± 2	35 ± 2	38 ± 2	77 ± 2	80 ± 3	80 ± 3	70 ± 1
3	30 ± 1	33 ± 1	36 ± 3	65 ± 3	66 ± 4	66 ± 3	58 ± 2
4	30 ± 1	32 ± 1	35 ± 2	55 ± 2	55 ± 3	57 ± 3	51 ± 2
5	29 ± 1	31 ± 1	34 ± 2	49 ± 2	49 ± 3	51 ± 1	46 ± 2

[a]Uncertainty ranges calculated as standard deviations from a minimum of n = 5 independent measurements.

dx.doi.org/10.1021/la3026655 | Langmuir 2012, 28, 15150−15159

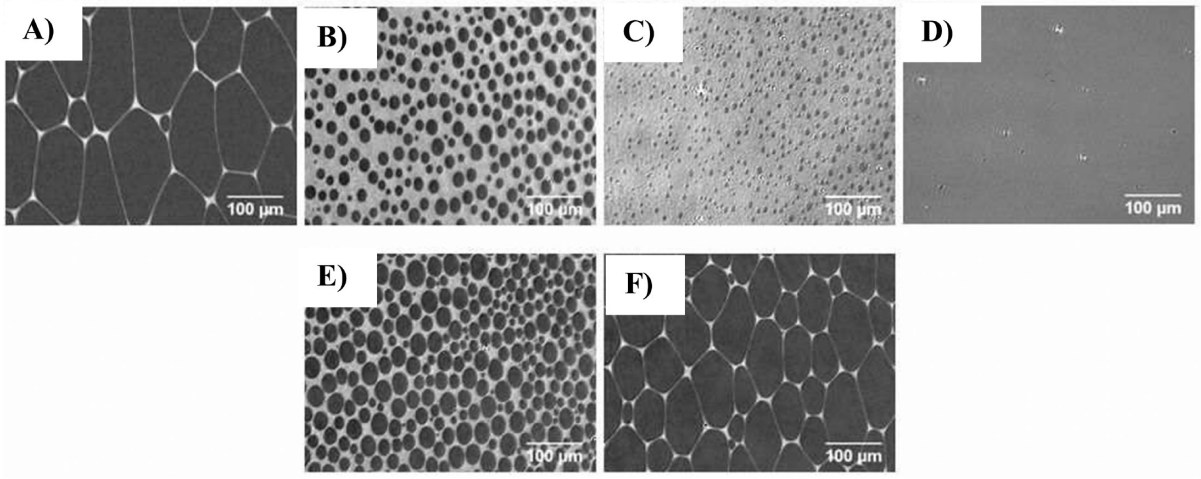

Figure 7. Series of consecutive Brewster angle micrographs (620 μm × 340 μm) of a χ_{C18F} = 0.5 mixed surfactant monolayer film collected during a compression−expansion cycle. (A) π = 2 mN/m; (B) π = 3 mN/m; (C) π = 4 mN/m; (D) π = 6 mN/m; (E) π = 4 mN/m; and (F) π = 3 mN/m. Corresponding video data is available in the Supporting Information.

it appears that in the case of the minimal model used in this study, such a mechanism is plausible.

In support of this model, we have measured a continuous series of BAM images for a χ_{C18F} = 0.5 mixed film during a single compression−expansion cycle (compression rate and expansion rate were equal and had a value of 20 mm·min^{-1}). A series of still images showing the results of these measurements are provided in Figure 7 (video of the data is available in the Supporting Information). As observed previously, the mixed films initially consisted of large, low-reflectivity regions (assigned as C18F) separated by strands of high-reflectivity (assigned as DPPC) material (Figure 7A). During compression, the relative size of the C18F domains decreased and the DPPC increased, corresponding to more close-packing of the different surfactant materials (Figure 7B, C). Ultimately, the C18F domains begin to vanish ("squeezed out"), leaving the film a uniform reflectivity (either the pure water subphase or a uniform layer of highly compressed DPPC) (Figure 7D). Upon re-expansion, the original domain structures reappear, and grow as a function of trough area, indicating the strong degree of reversibility of the cyclic process.

Further insight into both the time-scale of the surfactant respreading process and the extent of surfactant recovery can also be collected from these measurements. Upon film re-expansion after the initial compression, elapsed time between film collapse and the first appearance of circular domains was typically <10 s (determined through the frame rate of the CCD camera used for image collection). While complicated by the fact that the barriers are in constant motion during these experiments, the results are in overall good agreement with the surfactant spreading rate data described previously, and further suggests that any differences between the measured rates of surfactant spreading and surfactant respreading after compression are minimal for C18F. As an additional point, we note that the monolayer film structures in Figure 7 differ slightly for the compression and recompression at the same nominal trough area (e.g., panels B and F of Figure 7 are for the same trough area, but the images appear slightly different). This difference is the result of the irreversible loss of surfactant material during the re-expansion process.

In short, the results presented here suggest a mechanism of operation for this mixture that is consistent with the squeeze-out hypothesis, with the perfluorocarboxylic acid playing the role of the non-DPPC PS components, and the mixture as a whole exhibiting good surfactant recovery upon repeated cycling. While we emphasize that the system here is only intended as a simple, minimal model to describe behavior of mixed perfluorcarbon-DPPC PS films on a lung-fluid mimic subphase, the broad, general improvements in surfactant performance obtained through the use of perfluorinated surfactants suggests that this class of compounds holds significant potential for enhancing PS performance, and that further development and exploration of this class of additives for PS formulations is worthwhile.

4. CONCLUSIONS

The thermodynamic miscibility, film structures, spreading kinetics, and hysteresis response for a binary mixed C18F-DPPC monolayer system was investigated on a model lung fluid mimic subphase, with a view toward characterizing potential improvements to PS performance brought about by addition of a perfluorinated surfactant to DPPC. Under the subphase conditions explored here, the mixed films were fully immiscible, with the extent of miscibility depending modestly upon the composition of the mixed film. Comparison with related studies in the literature indicated that the subphase pH and salinity (via sodium ion binding) play a key role in regulating miscibility and mechanical properties of the resulting films. Highly structured, phase-separated monolayer films were observed at both the air−water and air−solid interfaces, and film compositions and the underlying molecular structure were determined through a combination of surface-sensitive microscopy techniques. With respect to performance of a potential PS mixture, addition of C18F to DPPC resulted in improved surfactant spreading rates and surfactant recovery, with minimal perturbations to overall film compressibility from the DPPC alone. The net overall improvement in performance resulting from the use of C18F in this model system suggests potential general utility of this class of molecules for enhancing PS performance in applied PS formulations.

dx.doi.org/10.1021/la3026655 | *Langmuir* 2012, 28, 15150−15159

■ ASSOCIATED CONTENT

Supporting Information

Standard deviations for mean molecular area measurements and excess Gibbs free energies of mixing. Characterization information (^{19}F-NMR) for the commercial C18F used in these experiments, before and after recrystallization. A Brewster angle microscope "movie" showing the response of a mixed monolayer film (χ_{C18F} = 0.5, compression rate of 67 mm·min^{-1}) at the air−water interface to a compression−expansion cycle. This material is available free of charge via the Internet at http://pubs.acs.org.

■ AUTHOR INFORMATION

Notes

The authors declare no competing financial interest.

■ ACKNOWLEDGMENTS

Financial support has been provided by the Natural Sciences and Engineering Research Council of Canada, the Canadian Foundation for Innovation, and the University of Saskatchewan. The Saskatchewan Structural Sciences Centre is acknowledged for providing access to confocal microscopy and NMR instrumentation. Dr. Keith Brown is acknowledged for assisting with NMR measurements.

■ REFERENCES

(1) Engelskirchen, S. *Curr. Opin. Colloid Interface Sci.* **2007**, *12* (2), 68−74.
(2) Rugonyi, S.; Biswas, S. C.; Hall, S. B. *Respir. Physiol. Neurobiol.* **2008**, *163* (1−3), 244−255.
(3) Zuo, Y. Y.; Veldhuizen, R. A. W.; Neumann, A. W.; Petersen, N. O.; Possmayer, F. *Biochim. Biophys. Acta, Biomembr.* **2008**, *1778* (10), 1947−1977.
(4) Serrano, A. G.; Perez-Gil, J. *Chem. Phys. Lipids* **2006**, *141* (1−2), 105−118.
(5) Hall, S. B.; Venkitaraman, A. R.; Whitsett, J. A.; Holm, B. A.; Notter, R. H. *Am. Rev. Respir. Dis.* **1992**, *145* (1), 24−30.
(6) Kobayashi, T.; Ohta, K.; Tashiro, K.; Nishizuka, K.; Chen, W.-M.; Ohmura, S.; Yamamoto, K. *J. Appl. Physiol.* **1999**, *86* (6), 1778−1784.
(7) Lu, J. J.; Cheung, W. W. Y.; Yu, L. M. Y.; Policova, Z.; Li, D.; Hair, M. L.; Neumann, A. W. *Respir. Physiol. Neurobiol.* **2002**, *130* (2), 169−179.
(8) Thomassen, M. J.; Antal, J. M.; Divis, L. T.; Wiedemann, H. P. *Clin. Immunol. Immunopathol.* **1995**, *77* (2), 201−205.
(9) Yu, L. M. Y.; Lu, J. J.; Chiu, I. W. Y.; Leung, K. S.; Chan, Y. W.; Zhang, L.; Policova, Z.; Hair, M. L.; Neumann, A. W. *Colloids Surf., B* **2004**, *36* (3−4), 167−176.
(10) Aydogan, N.; Uslu, B.; Tanaci, H. *J. Colloid Interface Sci.* **2011**, *360* (1), 163−174.
(11) Eftaiha, A. F.; Paige, M. F. *J. Colloid Interface Sci.* **2011**, *353* (1), 210−219.
(12) Krafft, M. P. *Adv. Drug Delivery Rev.* **2001**, *47* (2−3), 209−228.
(13) Nakahara, H.; Lee, S.; Krafft, M. P.; Shibata, O. *Langmuir* **2011**, *26* (23), 18256−18265.
(14) Kissa, E. *Fluorinated Surfactants and Repellents*, 2nd ed.; Marcel Dekker Inc.: New York, 2001; Vol. *97*.
(15) Krafft, M. P.; Goldmann, M. *Curr. Opin. Colloid Interface Sci.* **2003**, *8* (3), 243−250.
(16) Lau, C.; Anitole, K.; Hodes, C.; Lai, D.; Pfahles-Hutchens, A.; Seed, J. *Toxicol. Sci.* **2007**, *99* (2), 366−394.
(17) Lehmler, H. J.; Bummer, P. M. *J. Colloid Interface Sci.* **2002**, *249* (2), 381−387.
(18) Lehmler, H. J.; Bummer, P. M. *Biochim. Biophys. Acta, Biomembr.* **2004**, *1664* (2), 141−149.
(19) Hoda, K.; Kawasaki, H.; Yoshino, N.; Chang, C. H.; Morikawa, Y.; Sugihara, G.; Shibata, O. *Colloids Surf., B* **2006**, *53* (1), 37−50.
(20) Hoda, K.; Nakahara, H.; Nakamura, S.; Nagadome, S.; Sugihara, G.; Yoshino, N.; Shibata, O. *Colloids Surf., B* **2006**, *47* (2), 165−175.
(21) Courrier, H. M.; Vandamme, T. F.; Krafft, M. P.; Nakamura, S.; Shibata, O. *Colloids Surf., A* **2003**, *215* (1−3), 33−41.
(22) Hiranita, T.; Nakamura, S.; Kawachi, M.; Courrier, H. N.; Vandamme, T. F.; Krafft, M. P.; Shibata, O. *J. Colloid Interface Sci.* **2003**, *265* (1), 83−92.
(23) Nakahara, H.; Nakamura, S.; Kawasaki, H.; Shibata, O. *Colloids Surf., B* **2005**, *41* (4), 285−298.
(24) Nakahara, H.; Shibata, O. *J. Oleo Sci.* **2012**, *61* (4), 197−210.
(25) Yokoyama, H.; Nakahara, H.; Nakagawa, T.; Shimono, S.; Sueishi, K.; Shibata, O. *J. Colloid Interface Sci.* **2009**, *337* (1), 191−200.
(26) Yokoyama, H.; Nakahara, H.; Shibata, O. *Chem. Phys. Lipids* **2009**, *161* (2), 103−114.
(27) McConnell, H. M. *Annu. Rev. Phys. Chem.* **1991**, *42*, 171−195.
(28) Tsuji, M.; Inoue, T.; Shibata, O. *Colloids Surf., B* **2008**, *61* (1), 61−65.
(29) Goecke, C. M.; Jarnot, B. M.; Reo, N. V. *Chem. Res. Toxicol.* **1992**, *5* (4), 512−519.
(30) Gaines, G. L. *Insoluble Monolayers At Liquid−Gas Interfaces*; Interscience Publishers: New York, 1966.
(31) Eftaiha, A. F.; Brunet, S. M. K.; Paige, M. F. *J. Colloid Interface Sci.* **2012**, *368* (1), 356−365.
(32) Nakamura, S.; Nakahara, H.; Krafft, M. P.; Shibata, O. *Langmuir* **2007**, *23* (25), 12634−12644.
(33) Zuo, Y. Y.; Keating, E.; Zhao, L.; Tadayyon, S.; Veldhuizen, R.; Petersen, N. O.; Possmayer, F. *Biophys. J.* **2008**, *94*, 3549−3564.
(34) Wuestneck, R.; Perez-Gil, J.; Wustneck, N.; Cruz, A.; Fainerman, V. B.; Pison, U. *Adv. Colloid Interface Sci.* **2005**, *117* (1−3), 33−58.
(35) Taeusch, H. W.; Bernardino, d. l. S. J.; Perez-Gil, J.; Alonso, C.; Zasadzinski, J. A. *Biophys. J.* **2005**, *89* (3), 1769−1779.
(36) Pastrana, B.; Mautone, A. J.; Mendelsohn, R. *Biochemistry* **1991**, *30* (41), 10058−10064.
(37) Skoog, D. A.; Holler, J. F.; Nieman, T. A. *Principles of Instrumental Analysis*, 5th ed.; Nelson Thomson Learning: Toronto, ON, 1998.
(38) Thuenemann, A. F.; Schnablegger, H. *Langmuir* **1999**, *15* (16), 5426−5428.
(39) Yang, X. M.; Xiao, D.; Xiao, S. J.; Wei, Y. *Appl. Phys. A: Solids Surf.* **1994**, *A59* (2), 139−143.
(40) Korlach, J.; Schwille, P.; Webb, W. W.; Feigenson, G. W. *Proc. Natl. Acad. Sci. U.S.A.* **1999**, *96* (15), 8461−8466.